

## Thiol-Functionalized Undecagold Clusters by Ligand Exchange: Synthesis, Mechanism, and Properties

Gerd H. Woehrle and James E. Hutchison\*

Department of Chemistry and Materials Science Institute, 1253 University of Oregon, Eugene, Oregon 97403

Received September 19, 2004

Ligand exchange of phosphine-stabilized undecagold precursor particles,  $\text{Au}_{11}(\text{PPh}_3)_8\text{Cl}_3$ , with  $\omega$ -functionalized thiols provides a convenient and general approach for the rapid preparation of large families of thiol-stabilized, subnanometer ( $d_{\text{CORE}} \sim 0.8$  nm) particles. The approach permits rapid incorporation of specific functionality into the stabilizing ligand shell, is tolerant of a wide range of functional groups, and provides convenient access to new materials inaccessible by other methods. Mechanistic studies and trapping experiments give insight into the progression of the ligand exchange, providing evidence that the core size of the phosphine-stabilized undecagold precursor particles is preserved during ligand exchange. The optical properties of the thiol-stabilized nanoparticles depend strongly on the composition of the ligand shell, and a series of studies suggests that this dependence is a result of the ligand shell's influence on the electronic structure of the particle core, as opposed to a structural change within the nanoparticle core.

### I. Introduction

Metal nanoparticles with subnanometer core dimensions are of interest for fundamental studies and may be useful as building blocks for nanoscale devices because they are small enough to possess discrete electronic states<sup>1,2</sup> and can exhibit semiconductor-like electronic properties.<sup>3,4</sup> To study the fundamental properties of these nanoparticles and explore their use in specific applications, convenient access to ligand-stabilized nanoparticles possessing terminal functional groups is essential. Until recently, the lack of general synthetic strategies to introduce specific functionalities into the terminal positions of the ligand shell has limited detailed experimental investigations of the properties and reactivities of these materials.<sup>4–6</sup> Although a number of small transition

metal clusters with less than 20 core atoms have been studied for use as coordination complexes, catalysts,<sup>7</sup> and tagging reagents for biomolecules,<sup>8,9</sup> the vast majority of these clusters are stabilized by ligands (e.g., CO, Cp,  $\text{H}_2\text{O}$ , halides, etc.) that lack the chemical functionality needed to specifically bind the clusters to molecules, substrates, and surfaces.

Most examples of the introduction of functional groups into the ligand shell of subnanometer particles involve the use of functionalized triarylphosphines.<sup>10–13</sup> The synthesis of functionalized triarylphosphine-stabilized undecagold ( $\text{Au}_{11}$ ) clusters<sup>14</sup> typically requires an involved series of synthesis and separation steps, including phosphine-for-phosphine ligand exchange reactions,<sup>12</sup> postsynthetic transformations of functional groups,<sup>13</sup> and ion exchange chro-

\* Author to whom correspondence should be addressed. E-mail: hutch@uoregon.edu. Phone: 1-541-346-4228. Fax: 1-541-346-0487.

- (1) Collings, B. A.; Athanassenas, K.; Lacombe, D.; Rayner, D. M.; Hackett, P. A. *J. Chem. Phys.* **1994**, *101*, 3506–3513.
- (2) Schaaff, T. G.; Shafiqullin, M. N.; Khoury, J. T.; Vezmar, I.; Whetten, R. L.; Cullen, W. G.; First, P. N.; Wing, C.; Ascensio, J.; Yacaman, M. J. *J. Phys. Chem. B* **1997**, *101*, 7885–7891.
- (3) Chen, S.; Ingram, R. S.; Hostetler, M. J.; Pietron, J. J.; Murray, R. W.; Schaaff, T. G.; Khoury, J. T.; Alvarez, M. M.; Whetten, R. L. *Science* **1998**, *280*, 2098–2101.
- (4) Yang, Y.; Chen, S. *Nano Lett.* **2003**, *3*, 75–79.
- (5) Woehrle, G. H.; Warner, M. G.; Hutchison, J. E. *J. Phys. Chem. B* **2002**, *106*, 9979–9981.
- (6) Grant, C. D.; Schwartzberg, A. M.; Yang, Y.; Chen, S.; Zhang, J. Z. *Chem. Phys. Lett.* **2004**, *383*, 31–34.

- (7) (a) Hill, C. L.; Prosser-McCartha, C. M. *Coord. Chem. Rev.* **1995**, *143*, 407–455. (b) Pignolet, L. H.; Aubart, M. A.; Craighead, K. L.; Gould, R. A. T.; Krogstad, D. A.; Wiley, J. S. *Coord. Chem. Rev.* **1995**, *143*, 219–263. (c) Thimmappa, B. H. S. *Coord. Chem. Rev.* **1995**, *143*, 1–34. (d) Braunstein, P.; Rose, J. *Met. Clusters Chem.* **1999**, *2*, 616–677. (e) Pignolet, L. H. *Catal. Di- Polynucl. Met. Cluster Complexes* **1998**, 95–126.
- (8) Hainfeld, J. F. *Science* **1987**, *236*, 450–453.
- (9) Jahn, W. *J. Struct. Biol.* **1999**, *127*, 106–112.
- (10) Cariati, F.; Naldini, L. *Inorg. Chim. Acta* **1971**, *5*, 172–174.
- (11) Bartlett, P. A.; Bauer, B.; Singer, S. J. *J. Am. Chem. Soc.* **1978**, *100*, 5085–5089.
- (12) Jahn, W. *Z. Naturforsch., B: Chem. Sci.* **1989**, *44*, 1313–1322.
- (13) Reardon, J. E.; Frey, P. A. *Biochemistry* **1984**, *23*, 3849–3856.
- (14) Frey, P. A.; Frey, T. G. *J. Struct. Biol.* **1999**, *127*, 94–100.

matography.<sup>9,12,13</sup> The limited availability of functionalized phosphines and need for multistep transformations and separations limit the utility of these approaches as convenient and general routes to a diverse family of functionalized clusters. In addition, triarylphosphine-stabilized clusters exhibit only limited solution stability, especially in acidic solution, and are often prone to oxidative decomposition under ambient conditions.<sup>9,15</sup> A potential solution to enhancing the stability of these clusters involves stabilization through thiol ligands. Thiol-stabilized nanoparticles are known to exhibit higher stability than the phosphine-stabilized nanoparticles;<sup>16,17</sup> however, only a few examples of thiol-stabilized nanoparticles with subnanometer core dimensions are available.<sup>2,4,5,18</sup>

We recently investigated the ligand exchange of triphenylphosphine-stabilized undecagold (Au<sub>11</sub>) precursor particles ( $d_{\text{CORE}} \sim 0.8$  nm) with  $\omega$ -functionalized thiols as a reliable and convenient approach for producing functionalized, subnanometer gold particles.<sup>5</sup> Initial studies demonstrated successful ligand exchange of Au<sub>11</sub>(PPh<sub>3</sub>)<sub>8</sub>Cl<sub>3</sub> with a limited set (three) of different thiols but did not investigate the broader scope of this approach. In that study, we also noted a surprising dependence of the optical properties of the thiol-stabilized product particles on the thiol ligand used during ligand exchange but could not determine whether this was due to electronic effects of the ligand or to core size changes taking place during the exchange. Recent mechanistic work in our group showed that the ligand exchange of 1.5-nm phosphine-stabilized gold nanoparticles with thiols results in the loss of gold core atoms.<sup>17</sup> Although core size analysis by transmission electron microscopy (TEM) suggested that Au<sub>11</sub> core is preserved during ligand exchange, small changes in the number of core atoms are undetectable by TEM. Thus, we sought to investigate further whether core size changes occur during the ligand exchange of phosphine-stabilized Au<sub>11</sub> clusters with thiols and determine whether such changes could be responsible for the observed differences in the optical properties.

Here, we report the general features and scope of the ligand exchange reaction of Au<sub>11</sub>(PPh<sub>3</sub>)<sub>8</sub>Cl<sub>3</sub> with a wide range of  $\omega$ -functionalized thiols. The approach is convenient and tolerates organic- and water-soluble thiols with neutral or charged headgroups. Mechanistic studies of the exchange reaction provide strong evidence that the core size of the precursor particle remains unchanged during the ligand exchange. These studies show that, during the exchange of thiols for phosphines, the phosphine ligands are lost as free triphenylphosphine, demonstrating that undecagold particles follow a different mechanism for exchange reactions with thiols than their larger ( $d_{\text{CORE}} \sim 1.5$  nm) analogues.<sup>17</sup> Finally,

we show that the optical properties of the thiol-stabilized exchange products depend on the nature of the ligand shell and discuss possible causes for this dependence.

## II. Experimental Section

**Materials.** Hydrogen tetrachloroaurate was purchased from Strem and used as received. Dichloromethane was dried over calcium hydride and distilled prior to use. Chloroform was filtered through a plug of basic alumina prior to use to remove acidic impurities. Triphenylphosphine-stabilized undecagold particles, Au<sub>11</sub>(PPh<sub>3</sub>)<sub>8</sub>Cl<sub>3</sub> (**1**), were synthesized as described previously and had a core diameter of  $0.8 \pm 0.2$  nm.<sup>5</sup> 1-Azido-2,4-dinitrobenzene,<sup>19</sup> 2-(2-mercaptoethoxy)ethanol,<sup>20</sup> and 2-[2-(2-mercaptoethoxy)ethoxy]ethanol<sup>20</sup> were synthesized according to known procedures. ((2,4-Dinitrophenyl)imino)(triphenyl)phosphorane was prepared as described previously.<sup>17</sup> All other compounds were purchased from Aldrich and used as received.

**Analytical Procedures.** Nuclear magnetic resonance (NMR) spectra were collected on a Varian Unity Inova 300 MHz instrument equipped with a 4-channel probe (<sup>13</sup>C, 75.42 MHz; <sup>31</sup>P, 121.43 MHz). For <sup>1</sup>H and <sup>13</sup>C NMR, chemical shifts were referenced to the residual proton resonance of the solvent. For <sup>31</sup>P NMR spectroscopy, the spectra were referenced to H<sub>3</sub>PO<sub>4</sub> (external standard). X-ray photoelectron spectroscopy (XPS) was performed on a Kratos Axis HSi instrument operating at a base pressure of  $\sim 5 \times 10^{-9}$  mmHg using monochromatic Al K $\alpha$  radiation at 15 mA and 13.5 kV. Nanoparticle samples were drop-cast from solution onto clean glass slides. Samples were charge compensated, and binding energies were referenced to carbon 1s at 284.4 eV. UV-visible spectra were obtained on a Hewlett-Packard 8453 diode array spectrometer with a fixed slit width of 1 nm using 1-cm quartz cuvettes. Thermal gravimetric analysis (TGA) was performed on a TA Instruments Hi-Res TGA 2950 thermogravimetric analyzer under nitrogen atmosphere (flow rate 100 mL/min). Samples (1–2 mg) were deposited onto Al pans as powders or by drop-casting from dichloromethane and placed in the instrument until a stable weight was obtained prior to analysis. The samples were heated at a rate of 2 °C/min up to 100 °C, held at that temperature for 20 min to ensure complete solvent evaporation, and then heated to 500 °C at a rate of 1 °C/min. Transmission electron microscopy (TEM) was performed on a Philips CM-12 operating at 120 kV accelerating voltage. Samples were prepared by aerosol deposition of aliquots onto SiO<sub>2</sub>-coated 400-mesh Cu TEM grids (Ted Pella). The samples were dried under ambient conditions prior to inspection by TEM. Images were recorded and processed as described previously.<sup>21</sup>

**Synthetic Procedures. General Procedure for the Preparation of Organic-Soluble Undecagold Nanoparticles.** To a solution of  $5.0 \times 10^{-3}$  mmol **1** in dichloromethane/1-chlorobutane (1:3; 30 mL) was added 0.1 mmol of the organic-soluble thiol. The mixture was stirred rapidly at 55 °C until completion of the ligand exchange reaction. The reaction time depended on the incoming ligand and varied from 6 h for propanethiol up to 24 h for long-chain alkanethiols. Upon completion of the exchange reaction the solvent was removed in vacuo. To remove excess free ligand and byproducts, the crude material was dissolved in the minimum amount of ethanol or 2-propanol<sup>22</sup> and purified by gel filtration

(15) Schoenauer, D.; Lauer, H.; Kreibitz, U. *Z. Phys. D* **1991**, *20*, 301–304.

(16) (a) Brown, L. O.; Hutchison, J. E. *J. Am. Chem. Soc.* **1997**, *119*, 12384–12385. (b) Warner, M. G.; Reed, S. M.; Hutchison, J. E. *Chem. Mater.* **2000**, *12*, 3316–3320.

(17) Woehrle, G. H.; Brown, L. O.; Hutchison, J. E. *J. Am. Chem. Soc.* **2005**, *127*, 2172–2183.

(18) (a) Schaaff, T. G.; Whetten, R. L. *J. Phys. Chem. B* **2000**, *104*, 2630–2641. (b) Negishi, Y.; Tsukuda, T. *J. Am. Chem. Soc.* **2003**, *125*, 4046–4047.

(19) Bailey, A. S.; Case, J. R. *Tetrahedron* **1958**, *3*, 113–131.

(20) Woehrle, G. H.; Warner, M. G.; Hutchison, J. E. *Langmuir* **2004**, *20*, 5982–5988.

(21) (a) Brown, L. O.; Hutchison, J. E. *J. Phys. Chem. B* **2001**, *105*, 8911–8916. (b) Woehrle, G. H.; Hutchison, J. E.; Özkaz, S.; Finkle, R. G. Submitted for publication.

chromatography using Sephadex LH-20 (eluent, ethanol or 2-propanol; collect colored fraction).

**General Procedure for the Preparation of Water-Soluble Undecagold Nanoparticles.** An aqueous solution (15 mL) of 0.1 mmol of the water-soluble thiol ligand was added to a solution of  $5.0 \times 10^{-3}$  mmol **1** in  $\text{CHCl}_3$  (15 mL). The biphasic mixture was stirred rapidly at 55 °C until completion of the ligand exchange reaction which was monitored by the complete transfer of the colored nanoparticles from the organic to the aqueous phase. The reaction time depended on the incoming ligand and varied from 4 to 15 h. Upon completion of the exchange reaction the layers were separated, and the aqueous layer was washed with  $\text{CH}_2\text{Cl}_2$  ( $3 \times 10$  mL) and evaporated in vacuo. The crude material was redispersed in the minimum amount of water and purified by gel filtration chromatography using Sephadex LH-20 (eluent,  $\text{H}_2\text{O}$ ; collect colored fraction) to remove excess free ligand and byproducts. Alternatively, the crude products were dissolved in  $\text{H}_2\text{O}$  and purified by ultracentrifugation for 18 h at 340 000g. The nanoparticles formed a highly concentrated solution at the bottom of the centrifuge tube which could be separated from the supernatant.

**Synthesis of Carboxylic Acid-Functionalized, Thiol-Stabilized Undecagold Nanoparticles.** An aqueous solution (15 mL) of 0.1 mmol of the  $\omega$ -carboxyalkanethiol which was buffered to pH 8 using a 0.1 mM  $\text{KH}_2\text{PO}_4/\text{K}_2\text{HPO}_4$  buffer was added to a solution of  $5.0 \times 10^{-3}$  mmol **1** in  $\text{CHCl}_3$  (15 mL). The biphasic mixture was stirred rapidly at 55 °C until the transfer of the colored nanoparticles from the organic to the aqueous phase was complete. The reaction time depended on the incoming ligand and varied from 3 to 15 h. The layers were separated, and the aqueous layer was washed with  $\text{CH}_2\text{Cl}_2$  ( $3 \times 5$  mL) and evaporated in vacuo. The residue was dissolved in Nanopure water (10 mL) and precipitated by acidifying with 10% HCl to about pH 2. After the mixture was filtered, the residue was washed with 20 mL of 10% HCl, 20 mL of  $\text{H}_2\text{O}$ , and 5 mL of methanol. If higher purity is desired, this material can be dissolved in water and further purified by ultracentrifugation for 18 h at 340 000g. The nanoparticles form a highly concentrated solution at the bottom of the centrifugation tube which could be separated from the supernatant.

**NMR Monitoring of the Ligand Exchange between **1** and Thiols. General Procedure of Monitoring the Ligand Exchange between **1** and Hexanethiol by NMR.** All NMR experiments to monitor the ligand exchange reaction were conducted at 55 °C. Hexanethiol was placed in an NMR tube and dissolved in  $\text{DMSO-}d_6$ , and the solution was equilibrated in the NMR instrument to 55 °C. A single  $^1\text{H}$  NMR spectrum was obtained as a starting point for the reaction. The contents of the NMR tube were then added to a scintillation vial charged with **1**. The resulting mixture was quickly agitated until everything had dissolved and placed back into the NMR tube. The NMR tube was returned to the instrument and reshimmed, and spectra were collected at preset time intervals.

**Ligand Exchange between **1** and Excess Hexanethiol.** A solution of hexanethiol (2.8 mg,  $2.4 \times 10^{-2}$  mmol) in  $\text{DMSO-}d_6$  (0.6 mL) was added to **1** (5 mg,  $1.2 \times 10^{-3}$  mmol), and the reaction was monitored by either  $^1\text{H}$  NMR or  $^{31}\text{P}$  spectroscopy. The first spectrum was recorded at  $t_0 = 1$  min followed by spectra every 15 min for a total time of 12 h.

**Ligand Exchange between **1** and a Stoichiometric Amount of Hexanethiol (To Replace All Nanoparticle-Bound**

**Phosphines).** A solution of hexanethiol (1.5 mg,  $1.0 \times 10^{-2}$  mmol) in  $\text{DMSO-}d_6$  (0.6 mL) was added to **1** (5 mg,  $1.2 \times 10^{-3}$  mmol), and the reaction was monitored by  $^1\text{H}$  NMR spectroscopy. The first spectrum was recorded at  $t_0 = 1$  min followed by spectra every 15 min for a total time of 12 h.

**Ligand Exchange between **1** and Hexanethiol in the Presence of Excess  $\text{PPh}_3$ .** A solution of hexanethiol (1.5 mg,  $1.0 \times 10^{-2}$  mmol) and  $\text{PPh}_3$  (10 mg,  $4.0 \times 10^{-2}$  mmol) in  $\text{DMSO-}d_6$  (0.6 mL) was added to **1** (5 mg,  $1.2 \times 10^{-3}$  mmol), and the reaction was monitored by  $^1\text{H}$  NMR spectroscopy. The first spectrum was recorded at  $t_0 = 1$  min followed by spectra every 15 min for a total time of 12 h.

**Trapping Free  $\text{PPh}_3$  Using 1-Azido-2,4-Dinitrobenzene.** A solution of hexanethiol (2.8 mg,  $2.4 \times 10^{-2}$  mmol) and 1-azido-2,4-dinitrobenzene (10 mg,  $4.7 \times 10^{-2}$  mmol) in  $\text{DMSO-}d_6$  (0.6 mL) was added to **1** (5 mg,  $1.2 \times 10^{-3}$  mmol), and the reaction was monitored by  $^1\text{H}$  NMR spectroscopy. The first spectrum was recorded at  $t_0 = 1$  min followed by spectra every 1 min for a total time of 625 min.

### III. Results and Discussion

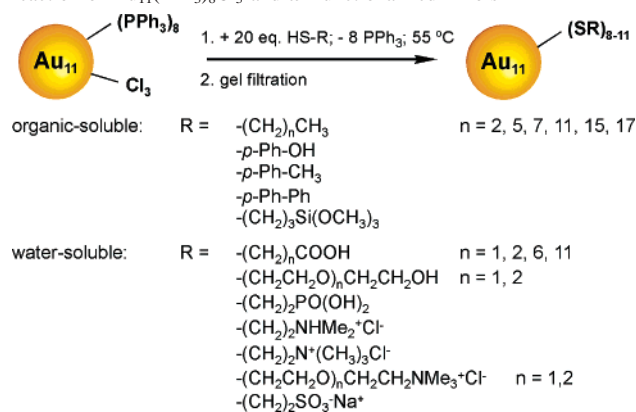
In the following section, we first describe the scope of the ligand exchange method to prepare functionalized, thiol-stabilized  $\text{Au}_{11}$  clusters from a common precursor particle. We will discuss ligand exchange reactions of  $\text{Au}_{11}(\text{PPh}_3)_8\text{-Cl}_3$  with a representative family of 22 methyl-terminated or  $\omega$ -functionalized thiols which include organic- and water-soluble alkane- or arenethiols with neutral or charged headgroups. Our results demonstrate the general nature of this approach and its tolerance to a wide range of important functional groups. The ease of preparation and convenient purification of the new materials synthesized by this method show its broad utility as a general route to functionalized  $\text{Au}_{11}$  particles.

A mechanistic investigation of the ligand exchange reaction by NMR spectroscopy is also described that gives fundamental insight into the progression of the exchange reaction and provides evidence that the number of core atoms is preserved during ligand exchange. These results are based upon product formation studies and trapping experiments. Unlike their 1.5-nm analogues, ligand exchange of  $\text{Au}_{11}(\text{PPh}_3)_8\text{-Cl}_3$  with thiols does not produce  $\text{AuCl}(\text{PPh}_3)$  as a byproduct, and all phosphine ligands are liberated from the nanoparticle as free  $\text{PPh}_3$ . Further evidence for the replacement of all phosphine ligands in form of  $\text{PPh}_3$  is demonstrated by experiments in which blocking of the ligand exchange was attempted through the addition of excess  $\text{PPh}_3$  to the reaction mixture.

In the final part of this section, we discuss the optical properties of the thiol-stabilized exchange products. This study is based upon UV-visible spectroscopy and suggests a strong dependence of the optical properties on the nature of the ligand shell.

**Scope of the Ligand Exchange Approach.** The phosphine-stabilized undecagold precursor particle,  $\text{Au}_{11}(\text{PPh}_3)_8\text{-Cl}_3$  (**1**), was synthesized using a modification of a procedure developed by Bartlett et al.<sup>11</sup> and had an average core size of  $0.8 \pm 0.2$  nm as determined by TEM.<sup>5</sup> Ligand exchange between **1** and alkane- or arenethiols was achieved by combining an excess of the thiol ( $\sim 20$  molar equiv) with a

(22) Most organic-soluble  $\text{Au}_{11}$  clusters can be dissolved in ethanol. Exceptions are clusters stabilized with long-chain alkanethiols such as octadecanethiol and hexadecanethiol. In these cases, less polar solvents such as 2-propanol must be used for chromatography. Alternatively, dichloromethane or chloroform can be used.

**Scheme 1.** Schematic Representation of the Ligand Exchange Reaction of Au<sub>11</sub>(PPh<sub>3</sub>)<sub>8</sub>Cl<sub>3</sub> and ω-Functionalized Thiols


nanoparticle solution in an appropriate solvent such as chloroform or water at 55 °C. To investigate the full scope of the ligand exchange approach, exchanges were carried out with a representative family of ω-functionalized thiols, including organic- and water-soluble alkane- or arenethiols with either neutral or charged headgroups (Scheme 1). All thiols tested were compatible with this approach, and only a few ligands (e.g., mercaptophenol, mercaptoethanesulfonic acid) required special reaction conditions to achieve complete exchange. In each case, the approach is generally applicable, leading to complete exchange of the original phosphine ligand shell.

As in the case of exchange reactions of 1.5 nm gold nanoparticles,<sup>17,23</sup> the reaction time depends on the thiol ligand used. The time increases as the chain length and bulkiness of the incoming ligand increase. However, the ligand exchange of Au<sub>11</sub> particles with thiols occurs only at elevated temperatures (~55 °C) and typically requires longer reaction times (approximately twice as long as in the case of 1.5 nm gold nanoparticles) due to the lower reactivity of Au<sub>11</sub> clusters.<sup>24</sup>

Ligand exchange reactions with organic-soluble thiols were carried out in a single organic phase and have been applied to a wide variety of alkane- and arenethiols (Scheme 1). Reaction times depend on the incoming ligand and vary from 6 h for propanethiol to 24 h for long-chain alkanethiols. Ligand exchange reactions with organic-soluble thiols were initially carried out in chloroform; however, this solvent leads to the rapid decomposition of the precursor cluster (**1**) and, thus, reduced yield. Filtering the chloroform through basic alumina immediately prior to use improved the yields, but partial decomposition of **1** still occurred.

To avoid the difficulties arising from particle decomposition in chloroform, a number of alternative reaction media were investigated, including alcohols, ethyl acetate, acetone, and dimethyl sulfoxide. Use of alcohols, ethyl acetate, or acetone eliminated decomposition of **1** but resulted in incomplete exchange due to precipitation of the particles during the exchange. In dimethyl sulfoxide, **1** showed

essentially no decomposition and the ligand exchange resulted in completely exchanged nanoparticles indistinguishable from those obtained in chloroform; however, the high boiling point of dimethyl sulfoxide makes its removal from the nanoparticle samples inconvenient. The best results were achieved using a mixture of 1-chlorobutane/dichloromethane (3:1) as the solvent. In this solvent system, ligand exchange resulted in completely exchanged thiol-stabilized Au<sub>11</sub> clusters with no decomposition of the precursor clusters.<sup>25</sup>

Water-soluble Au<sub>11</sub> clusters can also be prepared using this ligand exchange approach if a biphasic solvent system (water/CHCl<sub>3</sub>) is used in place of the organic solvent. As in the case of monophasic exchanges, the organic layer of the biphasic system can be replaced with a 3:1 mixture of 1-chlorobutane/dichloromethane; however, we did not find significant differences in yield using either alumina-filtered chloroform or 1-chlorobutane/dichloromethane as the solvent.<sup>26</sup> The pH of the aqueous layer was kept between 5 and 8 to avoid decomposition of the precursor particle under acidic conditions and prevent significant disulfide formation at higher pH. Typical reaction times for the biphasic ligand exchange reactions ranged from 4 h for ligand exchanges with (2-mercaptoethyl)trimethylammonium chloride up to 15 h using 2-[2-(2-mercaptoethoxy)ethoxy]ethanol. In exchange reactions involving thiols that contain ionizable headgroups (e.g., carboxylic acids), the pH must be raised to ensure complete deprotonation of the headgroups to avoid formation of insoluble material that can prevent complete exchange. In nearly all cases, the use of a phosphate buffer (pH = 8) as the aqueous layer yielded the best results.

The thiol-stabilized ligand exchange products can be purified either by solvent washes or, more conveniently, by gel filtration chromatography using Sephadex LH-20 resin. In practically every case, chromatography is more reliable, less wasteful, and faster than solvent washes. The use of the LH-20 resin allows for rapid purification of both organic- and water-soluble exchange products with a wide range of solvents, including alcohols, chlorinated organics, and water. The recovery of nanoparticle material from the column is nearly quantitative, and the support can be reused after sufficient rinsing.

To determine the chemical composition of the thiol-stabilized exchange products and ensure sufficient purity, we analyzed each exchange product using a combination of NMR, UV–visible spectroscopy, TEM, TGA, and XPS (Table 1). We used <sup>1</sup>H NMR spectroscopy to confirm the purity of each sample. The resonances associated with ligands bound to the gold core show significant line broadening.<sup>27</sup> The absence of sharp resonances indicates that excess free ligand and byproducts of the ligand exchange have been removed.<sup>25</sup> When nonaromatic thiols are used for the

(25) See Supporting Information.

(26) This is probably due to the rapid transfer of the exchanging particles from the organic to the aqueous phase.

(27) Terrill, R. H.; Postlethwaite, T. A.; Chen, C.-h.; Poon, C.-D.; Terzis, A.; Chen, A.; Hutchison, J. E.; Clark, M. R.; Wignall, G.; Londono, J. D.; Superfine, R.; Falvo, M.; Johnson, C. S. H., Jr.; Samulski, E. T.; Murray, R. W. *J. Am. Chem. Soc.* **1995**, *117*, 12537–12548.

(23) Hostetler, M. J.; Templeton, A. C.; Murray, R. W. *Langmuir* **1999**, *15*, 3782–3789.

(24) At temperatures below 40 °C, no ligand exchange is observed over a period of several days.

**Table 1.** Analytical Data for the Ligand Exchange Products

ligand	reaction time, h	$d_{\text{CORE}}^a$	$^1\text{H}$ NMR chem shift (ppm) and NMR solvent	S: Au ratio <sup>b</sup>	% ligand by mass <sup>c</sup>
HS(CH <sub>2</sub> ) <sub>2</sub> CH <sub>3</sub> <sup>d</sup>	6	0.8 ± 0.2 ( <i>N</i> = 1103)	1.15 (b), CDCl <sub>3</sub> 1.79 (b)	0.96	23.9
HS(CH <sub>2</sub> ) <sub>5</sub> CH <sub>3</sub> <sup>d</sup>	10	0.8 ± 0.2 ( <i>N</i> = 623)	0.90 (b), CDCl <sub>3</sub> 1.32 (b) 1.80 (b)	0.93	36.9
HS(CH <sub>2</sub> ) <sub>7</sub> CH <sub>3</sub> <sup>d</sup>	14	0.7 ± 0.2 ( <i>N</i> = 920)	0.88 (b), CDCl <sub>3</sub> 1.27 (b)	0.86	41.6
HS(CH <sub>2</sub> ) <sub>11</sub> CH <sub>3</sub> <sup>d</sup>	16	0.8 ± 0.3 ( <i>N</i> = 1032)	0.90 (b), CDCl <sub>3</sub> 1.25 (b)	0.91	47.1
HS(CH <sub>2</sub> ) <sub>15</sub> CH <sub>3</sub> <sup>d</sup>	20	0.8 ± 0.2 ( <i>N</i> = 810)	0.89 (b), CDCl <sub>3</sub> 1.27 (b)	0.87	53.8
HS(CH <sub>2</sub> ) <sub>17</sub> CH <sub>3</sub> <sup>d</sup>	24	0.8 ± 0.2 ( <i>N</i> = 623)	0.89 (b), CDCl <sub>3</sub> 1.26 (b)	0.89	56.1
4-mercaptophenol <sup>d</sup>	24 <sup>h</sup>	0.8 ± 0.2 ( <i>N</i> = 902)	7.23 (b), CD <sub>3</sub> OD	0.92	36.7
4-methylbenzenethiol <sup>d</sup>	20	0.7 ± 0.2 ( <i>N</i> = 718)	1.80 (b), CDCl <sub>3</sub> 7.11 (b)	0.89	35.7
4-mercaptobiphenyl <sup>d</sup>	20	0.8 ± 0.2 ( <i>N</i> = 512)	7.32 (b), CD <sub>2</sub> Cl <sub>2</sub>	0.86	44.8
HS(CH <sub>2</sub> ) <sub>3</sub> Si(OCH <sub>3</sub> ) <sub>3</sub> <sup>d</sup>	18	0.8 ± 0.3 ( <i>N</i> = 627)	3.40 (b), CD <sub>3</sub> OD 3.91 (b)	1.01	46.1
HS(CH <sub>2</sub> )COOH <sup>e</sup>	3	0.9 ± 0.2 ( <i>N</i> = 651)	3.10 (b), CD <sub>3</sub> OD	0.81	28.8
HS(CH <sub>2</sub> ) <sub>2</sub> COOH <sup>e</sup>	4	0.8 ± 0.2 ( <i>N</i> = 564)	3.30 (b), CD <sub>3</sub> OD	0.76	31.1
HS(CH <sub>2</sub> ) <sub>5</sub> COOH <sup>e</sup>	8	0.9 ± 0.3 ( <i>N</i> = 812)	1.21 (b), CD <sub>3</sub> OD 2.10 (b)	0.80	38.9
HS(CH <sub>2</sub> ) <sub>11</sub> COOH <sup>e</sup>	12	0.8 ± 0.2 ( <i>N</i> = 712)	1.31 (b), CD <sub>3</sub> OD 1.55 (b) 2.14 (b)	0.74	46.8
HS(CH <sub>2</sub> ) <sub>2</sub> O(CH <sub>2</sub> ) <sub>2</sub> OH <sup>f</sup>	10	0.8 ± 0.2 ( <i>N</i> = 1034)	3.73 (b), D <sub>2</sub> O	0.90	35.0
HS(CH <sub>2</sub> ) <sub>2</sub> O(CH <sub>2</sub> ) <sub>2</sub> O(CH <sub>2</sub> ) <sub>2</sub> OH <sup>f</sup>	15	0.8 ± 0.3 ( <i>N</i> = 832)	3.71 (b), D <sub>2</sub> O	0.83	41.5
HS(CH <sub>2</sub> ) <sub>2</sub> PO(OH) <sub>2</sub> <sup>f</sup>	7	0.9 ± 0.2 ( <i>N</i> = 591)	3.51 (b), D <sub>2</sub> O 3.27 2.26 (b)	1.02	39.7
HS(CH <sub>2</sub> ) <sub>2</sub> NMe <sub>2</sub> ·HCl <sup>f</sup>	9	0.9 ± 0.2 ( <i>N</i> = 704)	2.93 (b), D <sub>2</sub> O 3.55 (b) 3.80 (b)	0.74	35.1
HS(CH <sub>2</sub> ) <sub>2</sub> NMe <sub>3</sub> <sup>+</sup> Cl <sup>-f</sup>	4	0.8 ± 0.3 ( <i>N</i> = 923)	3.13 (b), D <sub>2</sub> O 3.52 (b)	0.84	38.0
HS(CH <sub>2</sub> ) <sub>2</sub> O(CH <sub>2</sub> ) <sub>2</sub> NMe <sub>3</sub> <sup>+</sup> Cl <sup>-f</sup>	8	0.8 ± 0.2 ( <i>N</i> = 689)	3.11 (b), D <sub>2</sub> O 3.62 (b)	0.79	44.2
HS(CH <sub>2</sub> ) <sub>2</sub> O(CH <sub>2</sub> ) <sub>2</sub> O(CH <sub>2</sub> ) <sub>2</sub> NMe <sub>3</sub> <sup>+</sup> Cl <sup>-f</sup>	9	0.8 ± 0.3 ( <i>N</i> = 834)	1.65 (b), D <sub>2</sub> O 3.18 (b)	0.92	49.7
HS(CH <sub>2</sub> ) <sub>2</sub> SO <sub>3</sub> <sup>-</sup> Na <sup>+.f,g</sup>	10	0.8 ± 0.2 ( <i>N</i> = 783)	3.42 (b), D <sub>2</sub> O 3.75 (b)	0.94	39.1

<sup>a</sup> Core diameter in nm (mean ± std dev) from analysis of representative TEM images. *N* refers to the number of particles measured. <sup>b</sup> Ratio obtained from quantification of the areas of the XPS signals. <sup>c</sup> Obtained from TGA analysis. <sup>d</sup> Synthesized according to the general procedure for the preparation of organic-soluble nanoparticles. <sup>e</sup> Synthesized according to the general procedure for the preparation of water-soluble nanoparticles but using a 3:1 KH<sub>2</sub>PO<sub>4</sub>/K<sub>2</sub>HPO<sub>4</sub> buffer (pH 8) as the aqueous phase. <sup>f</sup> Synthesized according to the general procedure for the preparation of water-soluble nanoparticles. <sup>g</sup> This material is obtained in a two-step synthesis as described elsewhere.<sup>5</sup> <sup>h</sup> The reaction is carried out in CH<sub>3</sub>Cl:MeOH (1:1).

exchange reaction,  $^1\text{H}$  NMR spectroscopy can also be used to confirm the completion of the ligand exchange (through the disappearance of the triphenylphosphine signals).

The core sizes of the exchange products were determined by analyzing representative TEM images for each nanoparticle sample.<sup>21</sup> The typical average core size of 0.8 ± 0.2 nm (*N* > 500) is the same as the core size of the phosphine-stabilized precursor particle **1** (see Table 1).<sup>25,28</sup> Because the optical properties of subnanometer gold clusters are highly sensitive to the number of core atoms,<sup>1,29,30</sup> determining the core size by UV–visible spectroscopy was

considered. However, UV–visible spectroscopy was not useful for probing the nanoparticle core size of the product particles because the optical properties of the nanoparticle are dependent on nature of the ligand shell, as described below.

The chemical composition of each exchange product was determined using a combination of XPS and TGA (Table 1). The absence of phosphorus (with the exception of mercaptoethanephosphonic acid-stabilized particles) in the XPS analysis confirmed complete ligand exchange and removal of all phosphine-containing byproducts within the detection limits of the instrument. For organic-soluble exchange products, XPS analysis also revealed the absence of chloride. Quantitative XPS analyses gave sulfur:gold ratios of organic-soluble exchange products ranging from 0.86:1.00 to 1.01:1.00, which correlate to ~9–11 thiols/nanoparticle. Water-soluble exchange products showed slightly lower sulfur:gold ratios of 0.74:1.00 to 1.02:1.00, corresponding

(28) The reported size dispersity of ~30% is due to the low contrast of the samples, the presence of touching particles, and irregularities in the support film which limits the accuracy of the analysis. Even in the case of the monodisperse, phosphine-stabilized undecagold precursor, size analysis gives 30% size dispersity.

(29) Hall, K. P.; Mingos, D. M. P. *Prog. Inorg. Chem.* **1984**, *32*, 237–325.

(30) Haebleren, O. D.; Chung, S.-C.; Stener, M.; Roesch, N. *J. Chem. Phys.* **1997**, *106*, 5189–5201.

to 8–11 thiols/nanoparticle. The sulfur:gold ratios of the exchange products obtained by XPS and TGA analyses are consistent with one another. The slightly lower thiol coverage of certain water-soluble exchange products could be due to some unexchanged chloride ligands or the presence of oxo ligands that could be produced by oxidation of some of the uncoordinated surface Au atoms during ligand exchange.

The ligand exchange approach is general and tolerates a surprisingly wide range of functional groups, using either a mono- or biphasic system. The approach produces functionalized Au<sub>11</sub> particles with technologically relevant headgroups such as alcohols for biological applications,<sup>31</sup> phosphonic acids and silanes for surface applications, and quaternary ammonium headgroups for self-assembly on DNA templates,<sup>20,32</sup> making this method potentially useful in many different research areas (e.g., nanoelectronics, biotagging, catalysis, etc.). In addition, the general nature of the approach, in combination with the ease of preparation and convenient purification, allows for the rapid preparation of large families of thiol-stabilized Au<sub>11</sub> particles.<sup>33</sup>

**Mechanism of the Ligand Exchange of Au<sub>11</sub>(PPh<sub>3</sub>)<sub>8</sub>Cl<sub>3</sub> and Thiols.** Only a few mechanistic investigations have been reported that provide information about the course and outcome of ligand exchange reactions of ligand-stabilized nanoparticles.<sup>17,23</sup> In this study, we investigated the mechanism for the replacement of the phosphine ligands by thiols to determine whether the core size is preserved during ligand exchange. Recent studies of the ligand exchange reaction of 1.5 nm triphenylphosphine-stabilized gold nanoparticles, “Au<sub>101</sub>(PPh<sub>3</sub>)<sub>21</sub>Cl<sub>5</sub>”, with alkanethiols showed that part of the phosphine ligand shell is replaced as AuCl(PPh<sub>3</sub>), leading to loss of core atoms.<sup>17</sup> The amount of AuCl(PPh<sub>3</sub>) produced is limited by the number of chlorides available in the original ligand shell which means that about 5% of the core atoms are lost as result of the exchange reaction.<sup>17</sup>

In the case of Au<sub>11</sub>(PPh<sub>3</sub>)<sub>8</sub>Cl<sub>3</sub>, a similar, partial replacement of the phosphine ligands as AuCl(PPh<sub>3</sub>) would result in the loss of three Au atoms and produce nanoparticles with a Au<sub>8</sub> core according to the number of chlorides in the original ligand shell. Since the optical properties of gold clusters with 6 to 13 core atoms are highly sensitive to the number of core atoms,<sup>1,29</sup> a change from a Au<sub>11</sub> core to a Au<sub>8</sub> during ligand exchange should lead to significant changes in the optical properties of the exchange products. These concerns led us to investigate the course of the ligand exchange reactions of the Au<sub>11</sub> core.

The progression of the ligand exchange reaction between **1** and hexanethiol was followed by in situ <sup>31</sup>P NMR spectroscopy to monitor the formation of phosphine-containing byproducts. To ensure complete exchange, the ligand

exchange between **1** and hexanethiol was carried out in an NMR tube at 55 °C using a 20-fold molar excess of the thiol. Deuterated DMSO was chosen as solvent to eliminate the decomposition of **1** to AuCl(PPh<sub>3</sub>) that occurs rapidly in CDCl<sub>3</sub>.<sup>34</sup> The exchange reaction was monitored until no more changes in the spectrum were observed (~12 h). At the end of the reaction, the <sup>31</sup>P NMR spectrum showed a major peak at 26.7 ppm, corresponding to triphenylphosphine oxide, and a small peak at 32.6 ppm, which was attributed to a trace amount of AuCl(PPh<sub>3</sub>), produced either by partial decomposition of the phosphine-stabilized precursor under the exchange conditions or as byproduct of the exchange reaction.<sup>34</sup> Signals for phosphines bound to the Au<sub>11</sub> core ( $\delta = 53.2$  ppm) or free PPh<sub>3</sub> ( $\delta = -5.5$  ppm) were not detected.

Triphenylphosphine oxide can either be formed by oxidation of the phosphine ligands on the nanoparticle surface (i.e., triphenylphosphine oxide is the leaving group of the ligand exchange) or is produced by the subsequent oxidation of liberated PPh<sub>3</sub> in solution.<sup>35</sup> To determine the origin of triphenylphosphine oxide, a trapping experiment was used to selectively probe for the presence of free PPh<sub>3</sub> in solution. Similar to a study reported previously,<sup>17</sup> we chose 1-azido-2,4-dinitrobenzene as the trapping reagent because it selectively undergoes a fast Staudinger reaction with PPh<sub>3</sub> to irreversibly form an iminophosphorane which is easily observable by NMR.<sup>36</sup> Triphenylphosphine oxide, produced as the leaving group of the ligand exchange reaction, would not result in the formation of iminophosphorane because the trapping reagent does not react with triphenylphosphine oxide. If triphenylphosphine oxide is formed by the oxidation of liberated PPh<sub>3</sub>, rapid formation of iminophosphorane would be observed. In addition, the amount of triphenylphosphine oxide will be greatly reduced because PPh<sub>3</sub> is rapidly removed from the mixture by the irreversible reaction with the trap.

When the ligand exchange reaction of **1** with an excess of hexanethiol is performed in the presence of 1-azido-2,4-dinitrobenzene, the formation of iminophosphorane is observed throughout the course of the ligand exchange reaction. Only trace amounts of triphenylphosphine oxide are produced in the presence of the trapping reagent. Since the formation of iminophosphorane only occurs in the presence of free PPh<sub>3</sub> in solution, this observation indicates that the phosphine ligands dissociate from the clusters as free PPh<sub>3</sub> and not triphenylphosphine oxide.

To investigate if the trace amount of AuCl(PPh<sub>3</sub>) observed during our initial NMR studies was formed as leaving group of the ligand exchange or was a result of the slow decomposition of **1** under the reaction conditions, we set up an experiment to block the ligand exchange by addition of

(31) Mrksich, M. *Chem. Soc. Rev.* **2000**, 29, 267–273.

(32) Warner, M. G.; Hutchison, J. E. *Nat. Mater.* **2003**, 2, 272–277.

(33) Thiol-stabilized exchange products show an increased stability towards heat, pH changes, and salt addition with respect to the phosphine-stabilized precursor particle **1**.<sup>5</sup> In addition, while water-soluble, phosphine-stabilized undecagold derivatives are being slowly oxidized when stored in solution for a few days or at low pH,<sup>9</sup> a similar sensitivity to oxidation has not been observed for **1** and the thiol-stabilized exchange products.

(34) In a control experiment, we found that Au<sub>11</sub>(PPh<sub>3</sub>)<sub>8</sub>Cl<sub>3</sub> produces only trace amounts of AuCl(PPh<sub>3</sub>) in DMSO-*d*<sub>6</sub> at 55 °C over the course of 12 h.

(35) In a control experiment, we found that PPh<sub>3</sub> is oxidized to triphenylphosphine oxide in DMSO-*d*<sub>6</sub> at 55 °C over the course of 2 h.

(36) (a) Triphenylphosphine oxide and gold-bound PPh<sub>3</sub> ligands do not react with the azide under identical conditions. (b) Staudinger, H.; Meyer, J. *Helv. Chim. Acta* **1919**, 2, 635–646.

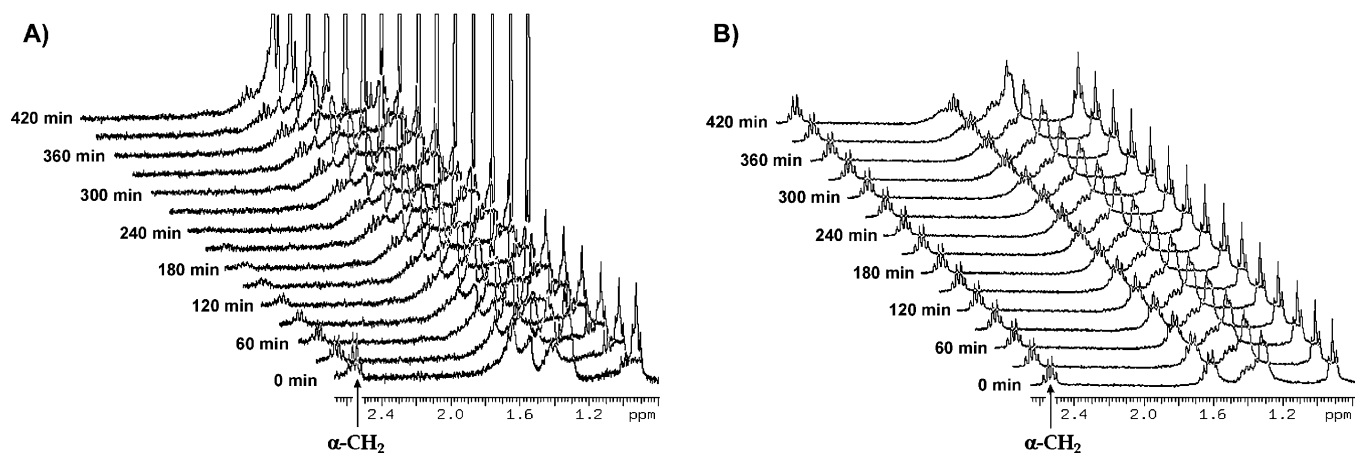


**Figure 1.** Evolution of the  $\alpha$ -methylene ( $\alpha$ -CH<sub>2</sub>) resonance of hexanethiol as a function of time for the ligand exchange of **1** with hexanethiol monitored by <sup>1</sup>H NMR spectroscopy. (A) The reaction was carried out in the presence a stoichiometric amount of hexanethiol to replace all of the ligands of **1**. The intensity of the  $\alpha$ -CH<sub>2</sub> resonance decreases over time as the thiols are exchanged onto the nanoparticle until it is broadened into the baseline after completion of the exchange. (B) The reaction was carried out under identical conditions as the experiment in (A) but in the presence of a 4-fold molar excess of PPh<sub>3</sub> over hexanethiol added prior to ligand exchange. The intensity of the  $\alpha$ -CH<sub>2</sub> resonance remains unchanged throughout the measurement, indicating complete blocking of the ligand exchange.

an excess of free PPh<sub>3</sub> to the ligand exchange mixture. Addition of excess of PPh<sub>3</sub> to the reaction mixture should only inhibit the loss of phosphine ligands as free PPh<sub>3</sub> but not their replacement as AuCl(PPh<sub>3</sub>). If AuCl(PPh<sub>3</sub>) was a leaving group of the ligand exchange, addition of excess PPh<sub>3</sub> should only lead to partial blocking of the ligand exchange.

Figure 1 shows the effect of addition of excess PPh<sub>3</sub> to the ligand exchange mixture on the progression of ligand exchange. The extent of ligand exchange can be monitored by the change in intensity of the <sup>1</sup>H NMR resonance for the  $\alpha$ -methylene protons (CH<sub>2</sub> protons closest to the sulfur) as the incoming thiol is exchanged onto the nanoparticle surface. In Figure 1A, the evolution of the  $\alpha$ -methylene proton peaks is shown as a function of time for a ligand exchange reaction between **1** and a stoichiometric amount of hexanethiol to completely replace all of the ligands of **1** (~11 molar equiv of thiol to Au<sub>11</sub>(PPh<sub>3</sub>)<sub>8</sub>Cl<sub>3</sub>). As the ligand exchange progresses, the intensity of the <sup>1</sup>H NMR resonance for the  $\alpha$ -methylene protons decreases until it broadens into the baseline toward the end of the exchange reaction. Approximately 200 min after the start of the ligand exchange, the resonance for the  $\alpha$ -methylene protons of the free thiol is not observable by NMR, indicating that all thiol is removed from solution and exchanged completely onto the nanoparticle.

Figure 1B shows the evolution of the  $\alpha$ -CH<sub>2</sub> protons over time for a ligand exchange reaction between **1** and stoichiometric hexanethiol in the presence of a 4-fold molar excess of PPh<sub>3</sub> over the amount of hexanethiol. In contrast to the exchange reaction without the addition of excess PPh<sub>3</sub> shown in Figure 1A, the intensity of the resonance the  $\alpha$ -methylene protons remains unchanged over the complete course of the experiment (~420 min) as indicated by the constant integration ratio of the  $\alpha$ -CH<sub>2</sub> protons and the terminal methyl protons. These results show that no thiol is removed from solution in the presence of an excess PPh<sub>3</sub>, indicating that the ligand exchange reaction is blocked completely. Complete inhibition of the ligand exchange by an excess of PPh<sub>3</sub> provides additional evidence that all phosphine ligands are

liberated from the nanoparticle as free PPh<sub>3</sub> because loss of the phosphine ligands as AuCl(PPh<sub>3</sub>) would lead to partial ligand exchange.<sup>17</sup> Therefore, the observed AuCl(PPh<sub>3</sub>) is most likely caused by partial decomposition of **1** under the reaction conditions and not a result of the ligand exchange.

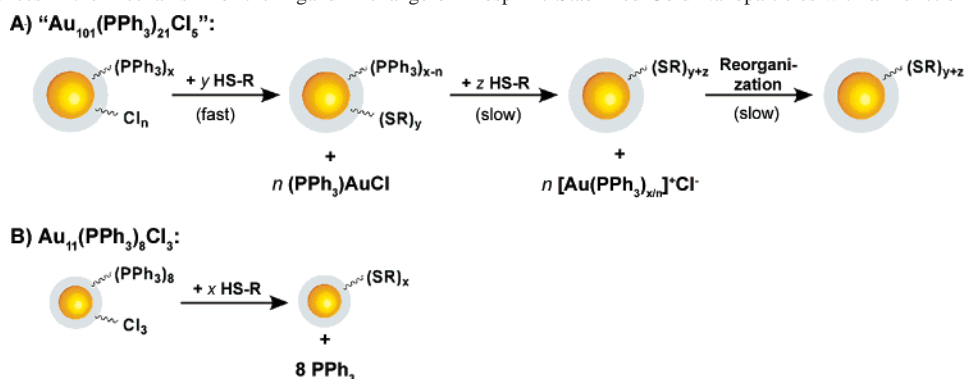
The experimental evidence from both the trapping studies and the blocking experiment suggests that the ligand exchange of Au<sub>11</sub> clusters with thiols follows a reaction mechanism different from the analogous exchange involving “Au<sub>101</sub>(PPh<sub>3</sub>)<sub>21</sub>Cl<sub>5</sub>”. The ligand exchange of “Au<sub>101</sub>(PPh<sub>3</sub>)<sub>21</sub>Cl<sub>5</sub>” with thiols proceeds in a three-stage mechanism in which about 25% of the phosphine ligands are replaced as AuCl(PPh<sub>3</sub>) during the initial stage of the ligand exchange.<sup>17</sup> The remaining phosphine ligands are removed in a subsequent stage by transfer to closely associated AuCl(PPh<sub>3</sub>) to form polyphosphine Au complexes. During the final stage of the exchange reaction the thiol ligand shell is being completed and reorganizes into a more crystalline state (Scheme 2A). In the case of Au<sub>11</sub>(PPh<sub>3</sub>)<sub>8</sub>Cl<sub>3</sub>, AuCl(PPh<sub>3</sub>) is not produced as a leaving group ligand exchange with thiols. Instead, the complete ligand shell is removed in form of free PPh<sub>3</sub> (Scheme 2B).

The results from our mechanistic studies provide strong evidence that the Au<sub>11</sub> core remains intact during the ligand exchange reaction, demonstrating the ability to control the core size of the product particles during the synthesis of the phosphine-stabilized precursor nanoparticles. Thus, it is possible to predict the core size of the product particles from the core size of the precursor.

The fate of the protons during the ligand exchange reaction remains unknown. The absence of a signal for the HS protons in the <sup>1</sup>H NMR spectra<sup>37</sup> of the thiol-stabilized exchange products suggest that the HS protons are being lost as a result of ligand exchange. It is unclear whether the HS protons are lost in form of H<sup>+</sup> or as H<sub>2</sub>. The NMR experiments did not provide any evidence for either one of the two species

(37) Hasan, M.; Bethell, D.; Brust, M. *J. Am. Chem. Soc.* **2002**, *124*, 1132–1133.

**Scheme 2.** Differences in the Mechanism for the Ligand Exchange of Phosphine-Stabilized Gold Nanoparticles with  $\omega$ -Functionalized Thiols



possibly due to the insufficient sensitivity. Another possibility is that the sulfur-bound hydrogen is transferred to an exiting ligand, e.g., chloride or triphenylphosphine, although these species were not observed in our experiments. Such a mechanism was recently shown for the exchange of thiols onto sulfide-stabilized Au nanoparticles in which intact thiols adsorb onto the nanoparticle surface and subsequently transfer hydrogen to a leaving ligand.<sup>37</sup>

**Optical Properties of the Thiol-Stabilized Product Particles.** Access to a large family of functionalized Au<sub>11</sub> particles provided by the ligand exchange method offers the opportunity to study the influence of the ligand shell on the optical properties. Although a number of Au<sub>11</sub> clusters have been prepared, their optical properties have not been studied in detail until recently.<sup>4–6</sup> Phosphine-stabilized Au<sub>11</sub> clusters have a characteristic UV–vis spectrum with maxima at 415, 385, and 301 nm which are only slightly sensitive to changes in the phosphine and halide ligands.<sup>9,29</sup> Storage of water-soluble Au<sub>11</sub> clusters at low pH or addition of oxidizing agents leads to noticeable shifts of the maxima to 425, 366, and 324 nm. These changes are completely reversible on addition of a small amount of a reducing agent (e.g., NaBH<sub>4</sub>) and are believed to reflect some rearrangement in the gold core.<sup>29</sup>

The optical properties of several thiol-stabilized Au<sub>11</sub> cluster also have been studied recently. Chen et al. investigated the electronic structure of dodecanethiol-stabilized Au<sub>11</sub> (Au<sub>11</sub>SC<sub>12</sub>) by voltammetric and spectroscopic measurements.<sup>4</sup> By comparing the voltammograms of Au<sub>11</sub>SC<sub>12</sub> with those of Au<sub>11</sub>(PPh<sub>3</sub>)<sub>7</sub>Cl<sub>3</sub>, they found that the band gap of the thiol-stabilized cluster is about 0.35 eV larger than for the phosphine-stabilized cluster. Under the assumption that the core dimensions remain unchanged during the exchange reactions, this observation was attributed to the stronger bonding of Au–S compared to that of Au–P(Cl). Furthermore, the authors found that thiol-stabilized Au<sub>11</sub> clusters (in contrast to the phosphine-stabilized precursor particles) exhibit photoluminescence and behave similarly to indirect band-gap semiconductors.

In the course of our studies, we observed distinct differences in the optical spectra of organic-soluble and water-soluble thiol-stabilized exchange products (Figure 2A). Undecagold particles stabilized with long-chain alkanethiols, such as octadecanethiol (ODT), have absorbance spectra

similar to those of the phosphine-stabilized precursor **1** with maxima at 318 nm, 330, 375, and 416 nm (due to interband transitions) but show an additional, broad peak at 690 nm. The latter peak was attributed to the excitonic transition of the subnanometer core<sup>4</sup> and is believed to reflect the semiconductor character of the Au<sub>11</sub> cluster.<sup>38</sup> In contrast to the spectrum of ODT-stabilized Au<sub>11</sub>, the spectra for water-

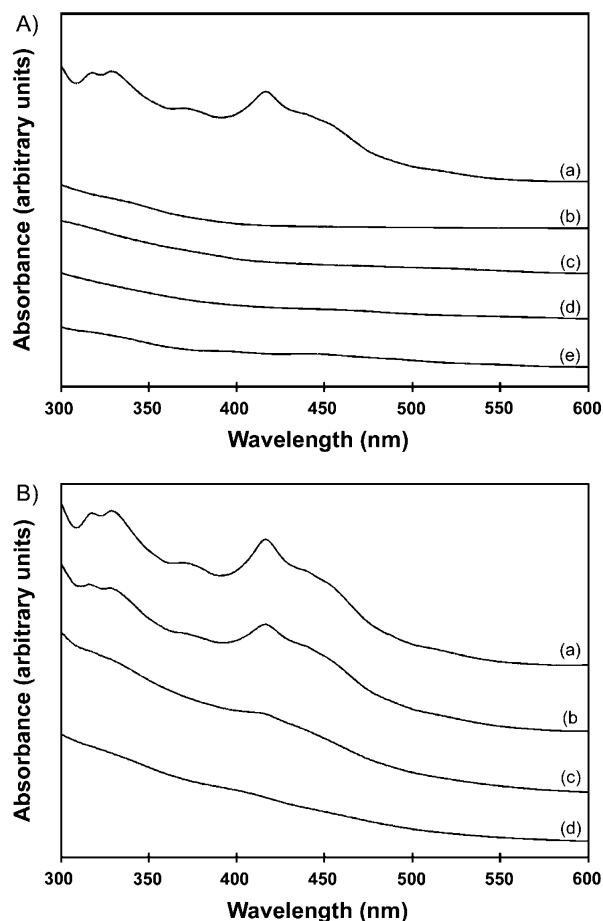


**Figure 2.** Dependence of the UV–visible spectra of thiol-stabilized Au<sub>11</sub> particles on the nature of the ligand shell. The spectra were normalized at 600 nm. (A) Comparison of the optical properties of organic-soluble and water-soluble Au<sub>11</sub> particles stabilized by (a) octadecanethiol, (b) mercaptoethanesulfonate, (c) mercaptopropionic acid, (d) mercaptoethanephosphonic acid, and (e) *N,N*-dimethylaminoethanethiol. (B) Dependence of the UV–visible spectra of organic-soluble Au<sub>11</sub> particles stabilized with straight-chain alkanethiols on the chain length. The stabilizing ligands were (a) octadecanethiol, (b) dodecanethiol, (c) octanethiol, and (d) hexanethiol.



soluble exchange products do not show defined peaks (Figure 2A).

A surprising trend was observed for the optical properties of organic-soluble, thiol-stabilized Au<sub>11</sub> particles when the chain length of the stabilizing alkanethiol ligand was decreased. Figure 2B shows the optical spectra of thiol-stabilized Au<sub>11</sub> particles with ligand shells composed of octadecanethiol, dodecanethiol, octanethiol, and hexanethiol. In this series of straight-chain alkanethiol-stabilized Au<sub>11</sub> particles, the defined maxima at 318, 330, and 416 nm broadened more and more with decreasing chain length of the thiol ligands. The Au<sub>11</sub>SC<sub>18</sub> particles showed the signature peaks of Au<sub>11</sub> particles observed in the absorbance spectrum of **1**; however, the optical spectra the Au<sub>11</sub> particles stabilized with the shortest thiol in the series, hexanethiol, resembled the optical spectra of water-soluble, thiol-stabilized Au<sub>11</sub> particles. This trend was unexpected considering the fact that the only known difference between the Au<sub>11</sub> clusters was the chain length of the stabilizing thiol ligand.

Possible explanations for the observed differences in the optical spectra are changes in core size and size dispersity. It is known that the optical and electronic properties of subnanometer gold clusters are strongly dependent on the number of core atoms.<sup>1,29,30</sup> Although our mechanistic studies suggested that no core atoms are lost during ligand exchange, it was possible that ligand exchange lead to ripening and rearrangement of nanoparticle core, resulting in polydisperse samples.<sup>39</sup>

To probe if the differences in core size and dispersity cause the different optical spectra of short-chain and long-chain thiol-stabilized Au<sub>11</sub> particles, we prepared Au<sub>11</sub>SC<sub>18</sub> particles by ligand exchange of hexanethiol-stabilized Au<sub>11</sub> particles, Au<sub>11</sub>SC<sub>6</sub>, with ODT and compared the absorbance spectrum with the one of Au<sub>11</sub>SC<sub>18</sub> prepared directly by ligand exchange of **1** with ODT. Thiol-for-thiol ligand exchanges have been shown to preserve the core size;<sup>23</sup> thus, the Au<sub>11</sub>-SC<sub>18</sub> particles prepared from Au<sub>11</sub>SC<sub>6</sub> particles should possess the same core dimensions as the Au<sub>11</sub>SC<sub>6</sub> precursor. Figure 3 shows the absorbance spectra of a sample of Au<sub>11</sub>-SC<sub>6</sub> particles before and after ligand exchange with ODT. Before ligand exchange, the spectrum was featureless, as is typical for undecagold particles stabilized by short-chain alkanethiols (Figure 3, trace a). After ligand exchange of this sample with ODT (Figure 3, trace b), the spectrum was similar to the spectrum of Au<sub>11</sub>SC<sub>18</sub> synthesized directly from Au<sub>11</sub>(PPh<sub>3</sub>)<sub>8</sub>Cl<sub>3</sub> with two distinct maxima at 322 and 416 nm (Figure 3, trace c).

The similarity between the spectra of the two Au<sub>11</sub>SC<sub>18</sub> samples prepared by the two methods suggests that both materials possess the same core size, suggesting that the initial thiol-for-phosphine ligand exchange of **1** as well as the subsequent thiol-for-thiol exchange reaction preserve the

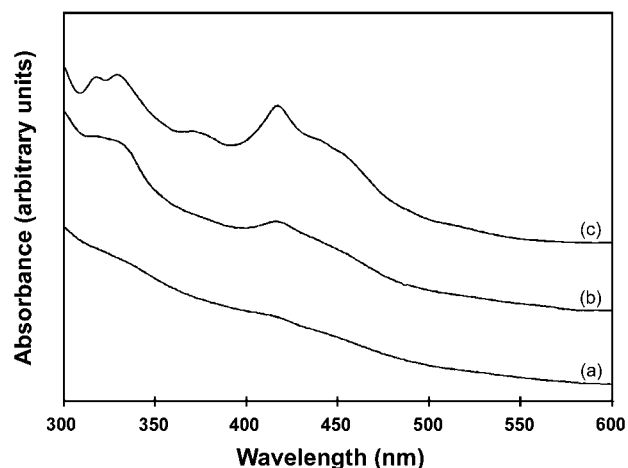


**Figure 3.** UV-visible spectrum of (a) organic-soluble Au<sub>11</sub> particles obtained by the ligand exchange of **1** with hexanethiol, (b) the thiol-stabilized Au<sub>11</sub> particles from (a) after a second ligand exchange with ODT, and (c) Au<sub>11</sub>SC<sub>18</sub> prepared directly by ligand exchange of **1** with ODT. All spectra were normalized at 600 nm.

undecagold core. The absorbances in the spectrum of Au<sub>11</sub>-SC<sub>18</sub> by ligand exchange of Au<sub>11</sub>SC<sub>6</sub> and ODT were not as defined as in the spectrum of Au<sub>11</sub>SC<sub>18</sub> synthesized directly from Au<sub>11</sub>(PPh<sub>3</sub>)<sub>8</sub>Cl<sub>3</sub>. A possible explanation for this observation is the presence of nanoparticles with mixed hexanethiol/ODT ligand shells. Thiol-for-thiol ligand exchange reactions of larger gold nanoparticles are typically incomplete and result in particles with mixed ligand shells.<sup>40</sup> Nanoparticles with mixed hexanethiol/ODT ligand shells might exhibit optical properties that lie between those of Au<sub>11</sub>SC<sub>18</sub> and Au<sub>11</sub>SC<sub>6</sub> particles.

Because the differences in the optical spectra appeared to be due to effects of the ligand shell and not to differences in core size and dispersity, we investigated if the different ligand shells of the nanoparticle samples affected the optical properties by influencing interparticle interactions and aggregation. Since these phenomena are concentration-dependent, the optical properties of long- and short-chain thiol-stabilized Au<sub>11</sub> particles were studied over a concentration range of 0.2–3.0 mM.<sup>41</sup> We found a linear relationship between the absorbance and the concentration, indicating that interparticle interactions or aggregation do not have noticeable effects on the optical spectra.<sup>25</sup>

We also investigated if solvation effects cause the observed difference in the optical properties. The optical properties of thiol-stabilized Au<sub>11</sub> particles were studied in various solvents including chloroform, ethanol, toluene, THF, and 1-chlorobutane, but we did not observe a noticeable dependence on the nature of the solvent in the investigated concentration range.<sup>25</sup>

Our optical studies indicate that during ligand exchange reactions of **1** with thiols no core size changes occur, confirming the results from the mechanistic investigation. We could further rule out that interparticle interactions and

(38) (a) Alivisatos, A. P. *J. Phys. Chem.* **1996**, *100*, 13226–13239. (b) Zhang, J. Z. *Acc. Chem. Res.* **1997**, *30*, 423–429.

(39) It is known that ligand exchange reactions can result in growth of the nanoparticles and changes in the size dispersity. For example, ligand exchange of 1.5-nm phosphine-stabilized Au nanoparticles with alkylamines leads to nanoparticle growth and ripening (see: Brown, L. O.; Hutchison, J. E. *J. Am. Chem. Soc.* **1999**, *121*, 882–883).

(40) Hostetler, M. J.; Green, S. J.; Stokes, J. J.; Murray, R. W. *J. Am. Chem. Soc.* **1996**, *118*, 4212–4213.

(41) The concentration range was chosen to include the concentration typically used for UV-visible spectroscopy of the nanoparticle samples.

solvation effects are responsible for the pronounced dependence of the optical properties of alkanethiol-stabilized Au<sub>11</sub> particles on the chain length of the thiol ligands. These results suggest that the nature of the thiol ligand has a direct influence on the electronic structure of the Au<sub>11</sub> core. Although it is known that thiols can act as electron acceptors decreasing the electron density of the gold core,<sup>4</sup> and possibly influencing the electronic structure of the gold core, the thiols used in this study have only minute differences in the electron acceptor properties. An improved understanding of these ligand effects would offer the opportunity to tune the optical properties of nanoparticles with the same core size through choice of the ligand shell.

#### IV. Conclusions

The ligand exchange chemistry of phosphine-stabilized Au<sub>11</sub> clusters with  $\omega$ -functionalized thiols is shown to be a powerful synthetic method that provides convenient access to a diverse family of functionalized Au<sub>11</sub> clusters. The general nature of this ligand exchange approach, in combination with the ease of preparation, makes it of broad utility. The approach is general and shows the high tolerance for a wide variety of functional groups. Mechanistic studies provided conclusive evidence that the Au<sub>11</sub> core of the precursor particle remains intact during ligand exchange and

showed that the ligand exchange of these particles follows a pathway different from that for ligand exchanges of larger gold nanoparticles such as "Au<sub>101</sub>(PPh<sub>3</sub>)<sub>21</sub>Cl<sub>5</sub>". Optical studies of the products show a strong dependence on the nature of the stabilizing thiol ligands. The ligand exchange approach offers the opportunity to study and tune systematically the optical and electronic properties of the nanoparticles through manipulation of the ligand shell.

**Acknowledgment.** Support for this work was provided by the National Science Foundation (Grant DMR-9705343). We thank Shaun Swartz for his assistance in synthesizing the propionic acid-stabilized undecagold particles and Lallie McKenzie and Darren Johnson for their assistance in designing and preparing the models used in generating the cover art.

**Supporting Information Available:** TEM images and NMR spectra of representative nanoparticle samples, thermal stability of **1** in 1:3 dichloromethane/1-chlorobutane, effects of the concentration on the optical properties of organic-soluble undecagold particles, and effects of the solvent on the optical properties of organic-soluble undecagold particles. This material is available free of charge via the Internet at <http://pubs.acs.org>.

IC048686+